

DOI:10.1002/ejic.201403183

Spring-Loaded Iron(II) Complexes as Magnetogenic Probes Reporting on a Chemical Analyte in Water

Corentin Gondrand,^{[a]†} Fayçal Touti,^{[a]†} Estelle Godart,^[a]
Yevgen Berezhansky,^[a] Erwann Jeanneau,^[b] Philippe Maurin,^[a] and
Jens Hasserodt*^[a]

Keywords: Cage compounds / Iron / Magnetic properties / Macrocyclic ligands / N ligands

A paramagnetic quality may be established in an aqueous sample if it contains a molecular probe that responds to the addition of a chemical analyte by turning from a diamagnetic state into a paramagnetic one (off–on). We explore here a stable, low-spin, binary iron(II) complex that stores so much potential energy that its transformation by the target analyte leads to its fragmentation into a high-spin complex despite the imposing strength of the chelate effect. The underlying ligand is a mixed aminal, the components of which can be freely varied to optimize response kinetics with the initial

probe stability preserved. With decreasing leaving-group character of the azole component, the probe stability improves, and the response kinetics diminish. An optimal arrangement can be found with a pyrazole paired with an electron-deficient aromatic carbaldehyde component (nitro substitution). The drastic electronic reversion associated with the reduction of the nitro group to an amino group is the principal reason for the observation of an initially stable probe that suffers swift fragmentation when reacted with a reductive analyte.

Introduction

Proving the presence of a particular chemical analyte in a sample is the *raison d'être* for the discipline of analytical chemistry but also plays an essential role in the rapidly expanding field of chemical imaging.^[1] Today, several physical detection modes serve this purpose, including electromagnetic waves (absorbance, fluorescence, phosphorescence, and interferometry), radioactivity [autoradiography, single-photon emission computed tomography (SPECT)], or electric currents (conductimetry). Although it has been relatively neglected, a magnetic mode of detection offers several advantages over classical modes. For example, the signal is not constantly emitted, as is the case for radioactive compounds, but is emitted only when an external magnetic field is applied. Also, the signal and the molecule from which it originates do not experience any fatigue, as is found for fluorescent or radioactive molecules. The signal emitted by the magnetic molecule is not attenuated during its passage through the sample, and finally, highly specific detection is

possible for several sample environments, including biological ones, that do not contain any other paramagnetic components. As eligible detection techniques, electron paramagnetic (EPR) spectroscopy may be cited as a direct method, and NMR spectroscopy may be cited as an indirect one (see Figure 4, b and c).

The design of molecular probes that actively respond to a chemical stimulus by changing the magnitude of their emitted signal is attractive because they offer better signal-to-background ratios and, thus, improved sensitivity. To the best of our knowledge, the examples of coordination compounds that respond to a change in their chemical composition by changing their magnetic properties do so only through gradual, reversible reactions.^[2–4] We introduced a new probe concept that is based on low-spin iron(II) binary complexes^[5–7] that undergo an irreversible reaction with the target analyte for high analyte specificity, optimal magnitude of signal change, and best adaptation to aqueous media. Our choice of the particular constitution of the complex has been motivated by the highly competitive nature of water as the solvent, the need to translate a chemical event into a readable signal, and the requirement to overcome the imposing strength of the chelate effect. We recently communicated a molecular probe that irreversibly establishes a paramagnetic quality (“on”) in an initially diamagnetic aqueous sample (“off”) upon the addition of a chemical analyte.^[8] It did so through fragmentation into three components once transformed by the target analyte. The fragmentation implied the cleavage of a five-membered chelate ring. This required the identification of a molecular

[a] Laboratoire de Chimie, UMR CNRS UCBL 5182, Université de Lyon–ENS de Lyon, 46, allée d'Italie, 69364 Lyon CEDEX 07, France
E-mail: jens.hasserodt@ens-lyon.fr
<http://www.ens-lyon.fr/CHIMIE/>

[b] Centre de Diffractométrie Henri Longchambon, Université de Lyon–UCBL, Site CLEA, Bâtiment ISA, 3ème étage
5, rue de la Doua, 69100 Villeurbanne, France

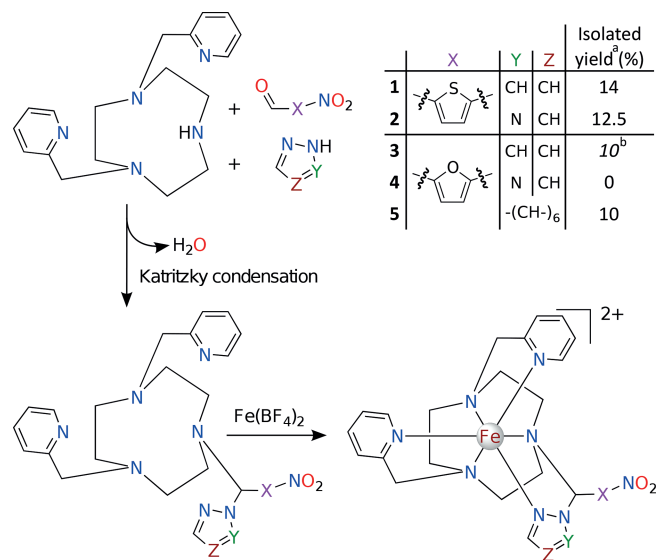
† These authors contributed equally.

Supporting information for this article is available on the WWW under <http://dx.doi.org/10.1002/ejic.201403183>.

moiety that stores much potential energy (spring-loading) without compromising the initial probe stability. Once chemically transformed by the target analyte, the resulting moiety should lead to swift fragmentation. Although the probe responded at neutral pH, near room temperature, and fairly rapidly, we were interested in whether its stability, response kinetics, or both could be improved. Here, we report on the expansion of this molecular system and explore the generality of its synthetic access and fragmentation mechanism. Thus, we varied two of the three components of the efficient condensation reaction that leads to the underlying hexadentate ligand of the probe. Five new iron(II) complexes were prepared, four of which were isolated, and two of which were obtained as crystals that led to X-ray structures. They exhibit electronic spectra, solution-phase magnetic moments, and bond angles and lengths similar to those of formerly reported representatives of this system. One of the new species, which displays a heteroaromatic analyte-reactive trigger moiety, shows faster response kinetics than those of the previously reported parent system. The present results make apparent the need for a compromise between probe stability in the absence of analyte and tendency to fragment in its presence. In this regard, a general trend can be derived for the variation of the azole portion.

Results and Discussion

The five target complexes were obtained through a convenient two-step, one-pot reaction (Scheme 1). This confirms the high versatility of this synthetic pathway, as suggested by previous studies.^[8]

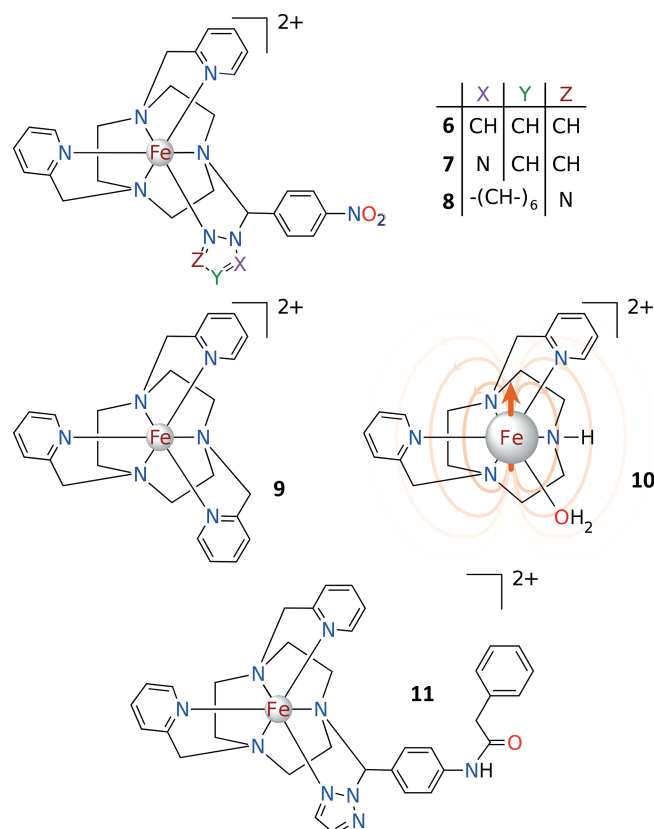


Scheme 1. Structure and synthesis of iron(II) complexes 1–5 (^a crystalline material unless stated otherwise; ^b powder).

The first step is the preparation of the hexadentate ligand, a mixed *N,N*-acetal (aminal), from three precursors. Two of them, a heteroaromatic aldehyde and an azole, are obtained from commercial sources; the third is the macro-

cyclic base triazacyclononane (tacn) bearing two picolyl pendent arms (dptacn).^[3,7] The condensation reaction is convergent and does not lead to any other amins aside from the targeted mixed aminal. The condensation was extensively explored by Katritzky et al. in the 1990s^[9] but never before applied to a secondary amine of such complexity, let alone a macrocyclic one.

The ligands that led to the previously reported **6**, **7**, and **8** (Scheme 2) were obtained in benzene under reflux with the help of a Dean–Stark apparatus to remove water and drive the reaction to completion. Unfortunately, when these conditions were applied to the present precursors, they systematically led to the degradation of the precursors. However, the present five ligands formed readily at room temperature in dichloromethane in the presence of activated molecular sieves. This success under milder conditions suggests that the heteroaromatic carbaldehydes based on thiophene (**1–2**) and furan (**3–5**) form thermodynamically more favorable mixed amins than those from benzaldehyde derivatives (**6–8**). As the amins were prone to rapid hydrolysis, as previously reported for **6–8**, their isolation was precluded. The quality of dptacn remains of utmost importance to the success of the condensation reaction. Indeed, poor conversion could often not be avoided even if the macrocycle was stored under an argon atmosphere. We suspect that the secondary amine moiety reacts with carbon dioxide and becomes deactivated.^[10] Therefore, to ensure the success of the reaction, the sample should be recent, preferably prepared freshly.



Scheme 2. Previously reported iron(II) complexes.^[12–14,8]

The second step consists of the trapping of the mixed aminals by in situ complexation with an iron(II) ion. The solution of the iron salt, which is added in a titration-like manner, has to be strictly anhydrous.^[11] All of the complexes, except **4**, are fairly stable in dichloromethane, acetonitrile, and water. Once the (swift) complexation is complete, the resulting complexes can be obtained in high purity by chromatography on a reversed-phase column (C18 cartridge) with a water/MeCN mobile phase, except for **4**, which decomposes under these conditions. The purification of the present complexes is somewhat more difficult than that of previously reported complexes **6–8** owing to the higher polarity of the furanylene and thiophenylene units compared to that of a phenylene moiety. Complexes **1**, **2**, **3**, and **5** could finally be obtained in isolated yields of 10 to 14%, as proven by mass spectrometry (Supporting Information) and elemental analysis. Complexes **1**, **2**, and **5** crystallized from concentrated MeCN solutions of the complex superposed by a layer of ether.

The crystals for **2** and **5** were suitable for X-ray diffraction analysis. The solved structures (Figures 1 and 2, Table S1 in the Supporting Information) confirm the mononuclear, binary nature of the complexes. The bond angles (listed in Tables 1 and 2) are in congruence with a quasi-octahedral coordination geometry. The two structures highlight the spatial separation of the trigger unit that is susceptible to the target analyte (nitro group) on the one side and the signal-generating coordination complex (the magnetogenic unit) on the other side.^[7]

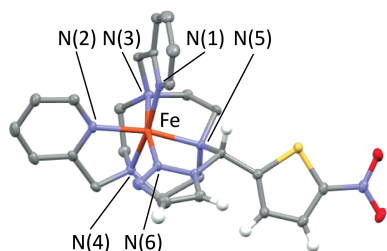


Figure 1. Thermal ellipsoid representation of the complex unit in **2** showing the quasi-octahedral geometry (ellipsoids drawn at 50% probability; the hydrogen atoms of the macrocycle and the two picolyl units and solvent molecules have been omitted for clarity).

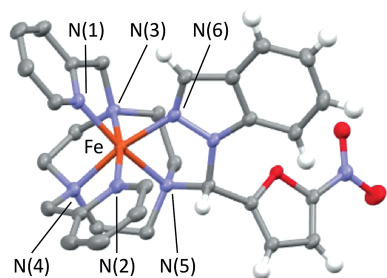


Figure 2. Thermal ellipsoid representation of the complex unit in **5** showing the quasi-octahedral geometry (ellipsoids drawn at 50% probability; the hydrogen atoms of the macrocycle and the two picolyl units and solvent molecules have been omitted for clarity).

Table 1. Selected bond lengths [Å] and angles [°] for **2**.

Fe–N(1)	1.976	N(1)–Fe–N(2)	93.03
Fe–N(2)	1.984	N(1)–Fe–N(3)	83.93
Fe–N(3)	1.985	N(1)–Fe–N(4)	169.53
Fe–N(4)	1.987	N(1)–Fe–N(5)	97.72
Fe–N(5)	2.015	N(1)–Fe–N(6)	94.15
Fe–N(6)	1.925	N(2)–Fe–N(3)	96.69
		N(2)–Fe–N(4)	83.17
		N(2)–Fe–N(5)	169.05
		N(2)–Fe–N(6)	95.02
		N(3)–Fe–N(4)	86.82
		N(3)–Fe–N(5)	86.57
		N(3)–Fe–N(6)	168.22

Table 2. Selected bond lengths [Å] and angles [°] for **5**.

Fe–N(1)	1.954	N(1)–Fe–N(2)	92.82
Fe–N(2)	1.970	N(1)–Fe–N(3)	84.86
Fe–N(3)	1.990	N(1)–Fe–N(4)	169.98
Fe–N(4)	1.990	N(1)–Fe–N(5)	96.31
Fe–N(5)	2.001	N(1)–Fe–N(6)	93.60
Fe–N(6)	1.922	N(2)–Fe–N(3)	97.38
		N(2)–Fe–N(4)	83.98
		N(2)–Fe–N(5)	170.40
		N(2)–Fe–N(6)	93.59
		N(3)–Fe–N(4)	86.73
		N(3)–Fe–N(5)	86.50
		N(3)–Fe–N(6)	168.92

The iron–nitrogen bond lengths (Table 3) are all slightly below 2.0 Å, as for the analogous structures of **6–8** and the parent diamagnetic complex **9** (FeTPTACN) reported previously. By comparison, the paramagnetic molecule **10** exhibits longer bond lengths of ca. 2.2 Å.^[14] This proves the firmly low-spin nature of the present complexes **1**, **2**, **3**, and **5** in the solid state. In addition, the triazole ring in **2** is bound to the aminal moiety through its N(2) nitrogen atom, as was the case for triazole-bearing **7**. However, **5** displays a nitrogen atom connectivity that may form to avoid steric clash between the indazole unit and the subsequent pendent picolyl group; this bonding fashion was also observed in the analogous benzotriazole-containing complex **8**.^[15–18]

Table 3. Comparison of average Fe–N bond lengths [Å] for **2**, **5**, and **6–9** in the solid state.

	Average Fe–N bond length	Reference
2	1.979	this work
5	1.971	this work
6	1.979	[8]
7	1.983	[8]
8	1.977	[8]
9	1.990	[13]
10	2.2	[14]

The electronic spectra of all isolated complexes have been acquired for crystalline samples when possible (see Table 4 and the Supporting Information). The spectra are characterized by the presence of a π – π^* band (column A in Table 4) at $\lambda \approx 250$ nm (presence of picolyl groups) and a metal-to-ligand charge-transfer band (MLCT) at $\lambda \approx 400$ nm. These wavelengths and their associated molar ex-

tion coefficients (ϵ) suggest a fully low-spin state for these iron(II) complexes, as illustrated by the similarity with the spectrum of the model compound **9**.^[13,19] Complexes **1**, **3**, and **6**, which contain a pyrazole moiety, exhibit a splitting of the MLCT that might be explained by the dissymmetric substitution/coordination motif; by comparison, the other complexes, which contain a triazole unit, show a single, shoulderless band. Complexes **5** and **8**, which contain indazole and benzotriazole units, respectively, give rise to bands of a more complex shape. All of the newly prepared complexes also exhibit an additional π - π^* band (labeled B in Table 4) at $\lambda \approx 300$ nm owing to the presence of a nitrothiophenyl or nitrofuranyl unit.^[20] This band is absent in the spectra of **6**, **7**, and **8** because they comprise a phenylene unit that habitually absorbs below 200 nm.

Table 4. Major UV/Vis spectroscopy data [λ_{\max} , nm (ϵ , $M^{-1}cm^{-1}$)] of **1–3** and **5–9** in aqueous solution.

	π - π^* A	π - π^* B	MLCT	Reference
1	254 (12207)	313 (12662)	393 (8419), 412 (8258)	this work
2	254 (8148)	307 (6637)	389 (7470)	this work
3	254 (7968)	304 (9352)	394 (5575), 412 (5558)	this work
5	252 (13830)	302 (11279)	402 (11658)	this work
6	255 (15859)	–	397 (6657), 416 (6697)	[8]
7	250 (14231)	–	391 (7559)	[8]
8	255 (21935)	–	436 (12417)	[8]
9	248 (3184)	–	432 (11970)	[6,19]
10	237 (3179)	–	329 (2870)	[6]

In view of our principal interest in aqueous media as the sample environment (and the magnetogenic response to the presence of a chemical analyte therein), we determined the magnetic status of our target complexes in solution. The 1H NMR spectra of **1**, **2**, **3**, and **5** in D_2O (Supporting Information) are all in congruence with their diamagnetic nature, as all peaks lie in the usual 10 ppm window. The method introduced by Evans (see Table 5 and the Supporting Information) confirms this hypothesis and furnishes values for the effective magnetic moment (μ_{eff}) of ca. $0.8 \mu_B$ at 293 K.^[21,22] This corresponds to the result for model low-spin complex **9** (FeTPTACN) and indicates the preservation of the low-spin status in solution.^[6] By contrast, **10** (Scheme 2), the ultimate product of our desired activation process, exhibits a moment of $5.5 \mu_B$, as determined previously (Table 5).^[6] Thus, it can be concluded that our choice of the macrocycle tacn as the base system in conjunction with the presence of three pendent arms with an imine-type nitrogen atom and six five-membered chelate

Table 5. Magnetic moments μ_{eff} [μ_B] of **1–3**, **5**, and **9** in aqueous solution at 293 K.

	μ_{eff}	Reference
1	0.74	this work
2	0.89	this work
3	0.75	this work
5	0.66	this work
9	0.9	[6]
10	5.5	[6]

rings reliably leads to completely low-spin iron(II) complexes (off status)^[6] in a solvent as competitive as water.^[7]

Three prerequisites for good probe performance should be put forward: (1) robustness (stability in the absence of the analyte), (2) efficient chemical conversion by reaction with the analyte, and (3) swift fragmentation of the initial product as a result of analyte conversion. These qualities were verified by UV/Vis spectroscopy and mass spectral monitoring.

We first tested the stability of the complexes. The robustness of this line of iron(II) complexes is quite dependent on the composition of the aqueous medium, as we observed for our previously reported probe **11** (Scheme 2). Complex **11** is stable in blood serum^[8] but slowly degrades in phosphate-buffered saline (PBS, pH 7.4; UV spectroscopic data in the Supporting Information). When samples of **1**, **2**, **3**, and **5** in 50 mM PBS (pH 7.4) at 37 °C were monitored by UV spectroscopy (Figure 3) over 2 h, the spectra of **1**, **3**, and **5** showed practically no evolution over time (2 h), where those for **2** indicate degradation. Mass spectral monitoring at the same time points confirms this behavior (Supporting Information). As a general trend, maximum stability in the phenylene series can only be obtained with the strongest electron-withdrawing group (nitro) at the *para* position (**6–8**), whereas a less definite electronic effect (acylated amine), as found in **11**, weakens the construction. When moving from the phenylene series to heteroaromatic spacers in the present study, this trend appears to occur slightly earlier and renders even a nitro-substituted thiophene derivative (**2**) unstable. Therefore, only **1**, **3**, and **5** were retained for subsequent analysis.

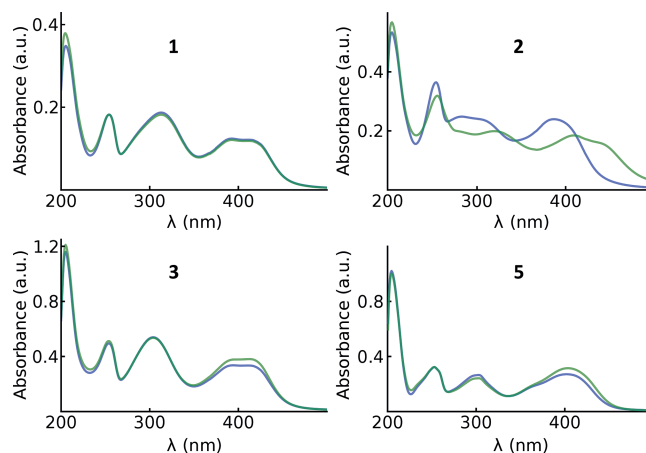


Figure 3. Monitoring by UV/Vis spectroscopy of the stability of **1–3** and **5** in PBS (50 mM, pH 7.4) at 37 °C. Blue line: freshly dissolved sample. Green line: after 2 h incubation.

The efficiency of probe conversion was now assessed. The chemical analyte used here, molecular hydrogen in the presence of a solid-state catalyst (Pd-C 10%), is known to reduce aromatic nitro groups very quickly. We initiated probe conversion over 10 min of catalytic hydrogenation, removed the catalyst by filtration, and analyzed the crude solution immediately. Although **1**, **3** and **5** all showed clean reduction to the corresponding amino derivatives (as dem-

onstrated in Figures S20–S22), the UV/Vis (Figure 4, a) and MS spectra (Figures S23 and S24) for the amines resulting from **1** and **5** did not evolve over 2 h. On the other hand, the mass spectral signal corresponding to the amine intermediate of **3** disappears over 1 h (Figure 4, a and Supporting Information, Figure S25). The monitoring of the same process by UV/Vis spectroscopy (see Supporting Information) yielded a half-life of 8.6 min, which reflects slightly faster response kinetics than previously observed for probe **7** (25 min) under the same conditions. To determine the fate of the organic ligand upon complete disappearance of the amine derivative of **3**, the sample was brought to pH 13 and extracted with dichloromethane. The ^1H NMR spectrum of the extract solely exhibits signals (see Figure S28) corresponding to the presence of the dptacn base system and pyrazole; the signals of the furan unit are absent, a fact that is in congruence with the claims by other authors that it suffers degradation.^[23–25]

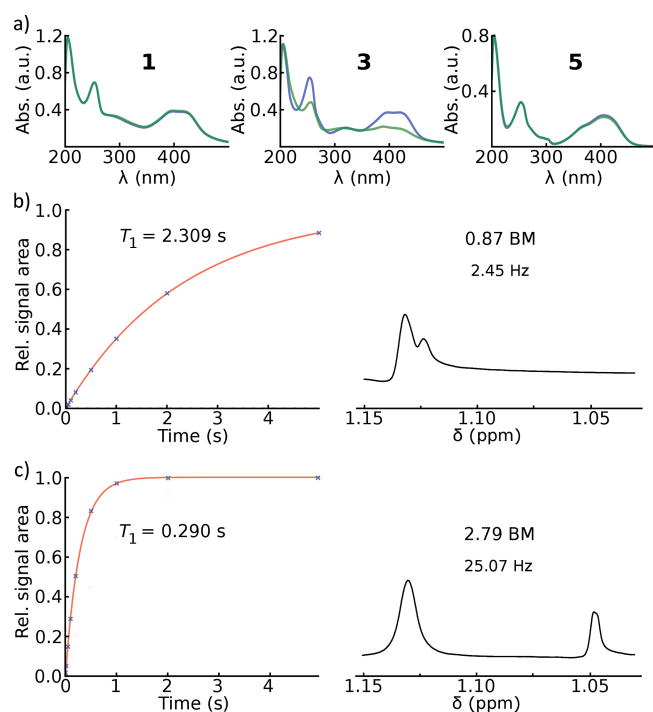
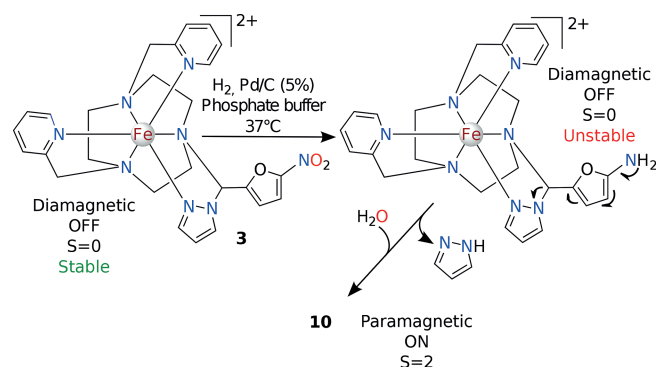


Figure 4. Monitoring of the fragmentation of the intermediates resulting from the activation of **1**, **3**, and **5**. (a) Monitoring by UV/Vis spectroscopy of a 0.05 mM PBS solution (0.02 mM for **5**; pH 7.4); blue line: immediately after activation; green line: after 2 h incubation at 37 °C; (b, c) T_1 monitoring (left, 4 mM) and ^1H NMR spectra (right, 6 mM) of **3** in PBS before (b) and after (c) activation.

The longitudinal relaxation time (T_1) of the water hydrogen nuclei of a sample of **3** before and after activation was monitored with an NMR spectrometer (Figure 4, b). The initial value was 2.3 s, which is somewhat below the value for pure water; this can be explained by the powder quality of **3** and the presence of traces of impurities, which can have a significant impact on relaxation times, as we have experienced in other contexts. After the complete disappearance of the amine resulting from the reduction of **3**, the relaxation time of 290 ms suggests that the species re-

sulting from the fragmentation of **3** is paramagnetic. Indeed, the application of the Evans NMR method to the initial sample and the totally converted sample of **3** furnished magnetic moments of 0.87 and 2.79 μ_{B} , respectively. This demonstrates that **3** is an effective magnetogenic probe, whereas **1**, **2**, and **5** are not. By analogy with the previously reported probe **7**, the amine derivative of **3** loses a pyrazole unit to afford a characteristic 5-methylene-furan-2-(5H)-imine intermediate (Figure S25), which is hydrolyzed to **10** (Scheme 3).^[26] The final value of 2.79 μ_{B} can be explained by the accumulation of one full equivalent of free pyrazole in the sample, which partially coordinates to the iron center at the newly established free coordination site and, thus, effectively renders a limited proportion of complex **10** low-spin. This phenomenon can be expected to be much less pronounced in a real-world setting, as concentrations should remain significantly below the 6 mM that were used for the present measurements.



Scheme 3. Mechanism of magnetogenic response by **3** in analogy with **7** (50 mM PBS, pH 7.4).^[8]

As a general trend, the increased stability of the initial probe and the lack of susceptibility to fragmentation after conversion when moving from triazole to pyrazole derivatives is confirmed. This may be explained by the significantly higher pK_a value of pyrazole ($\text{pK}_a = 14$) compared to that of triazole ($\text{pK}_a = 10$) and, thus, its much poorer leaving-group character. The move from a nitrated phenylene unit in our former report to a nitrated thiophenylene or furanylene moiety in the present work causes the overall probe stability to diminish. This may explain why the stability and fragmentation speed of **3** (combination of a furanylene and a pyrazole unit) and that of previously reported **7** (combination of a phenylene and a triazole unit) are similar. Two factors may also explain the higher tendency of heteroaryl complexes to fragment compared to that of the formerly reported phenylene ones: (a) the heterocycles exercise less steric hindrance owing to their cycle size (five-membered) and the absence of an α substituent on one of the atoms flanking the atom connected to the aminal carbon atom; this should allow the adoption of larger dihedral angles and, thus, the attainment of lower-lying transition states of elimination (see Scheme 3); (b) the heteroaryl spacers benefit from higher electron density than that of a phenylene moiety, and this may lower the energy content of the intermediate resulting from azole elimination.

Conclusions

We have explored five binary, low-spin iron(II) complexes of significant structural variation for their ability to fragment in aqueous media into a high-spin complex if their aromatic nitro group is reduced to an amino group by catalytic hydrogenation. Four of the complexes gave rise to complexes that can be isolated. Although two of the pyrazole derivatives are inert toward fragmentation, the one containing the nitrofuranylene trigger moiety fragments readily once reduced. It does so at a rate somewhat faster than that of the previously reported reference compound. This work has demonstrated that the unusual synthetic access to this system can be further generalized and extended to heteroaryl carbaldehydes. The spring-loaded trigger unit (the mixed amination) makes the system rare in its capacity to fragment and, thus, overcome the strong chelate effect necessary for the observation of the initially stable probe structures. However, true aqueous robustness for this line of iron(II) complexes can only be found with a nitro substituent as the trigger group; the drastic inductive reversion associated with the reduction of the nitro group to an amino group is the principal reason for the observation of an initially stable probe that suffers swift fragmentation when reacted with a reductive analyte. Although catalytic hydrogenation served as a model analyte, other analytes such as dithionite^[27,28] or nitroreductase/NADH^[26,29–32] convert similar probes just as well. The latter analyte is habitually the target in the identification of hypoxia as a biomarker of cancer metastasis.

Experimental Section

General: Dry dichloromethane (DCM) was obtained by drying commercially available DCM for 24 h with thermally activated molecular sieves (3 Å, sieves activated by 24 h heating at 315 °C). Routine chemicals were supplied by Sigma–Aldrich Co., Alfa Aesar, Acros Organics, and Tokyo Chemical Industries and used without further purification. All ¹H NMR spectra were acquired at 297 K with a Bruker AVANCE 300 spectrometer (300 and 75 MHz for ¹H and ¹³C, respectively). Chemical shifts (δ) are reported in ppm and referenced to residual solvent signals. Unit masses were measured by direct injection of samples into the mass analyzer of an Agilent Technologies 1260 Infinity LC–MS system running in electrospray ionization (ESI) mode. UV/Vis spectra were recorded with a UV-670 UV/Vis spectrophotometer (JASCO Inc.).

Complex 1: In a 50 mL flask, activated 3 Å molecular sieves (2.5 g), 1*H*-pyrazole (131 mg, 1.93 mmol, 1.5 equiv.), and 5-nitrothiophene-2-carbaldehyde (303 mg, 1.93 mmol, 1.5 equiv.) were added to a solution of 1,4-bis(pyridin-2-ylmethyl)-1,4,7-triazacyclononane^[6] (400 mg, 1.28 mmol) in dry dichloromethane (15 mL). This mixture was stirred under an inert atmosphere for 15 h at room temperature. An anhydrous acetonitrile solution of [Fe(BF₄)₂·(CH₃CN)₆]^[11] was then added in a titration-like manner. The resulting solution was filtered, and the filtrate was concentrated in vacuo. The residue was dissolved in a minimal volume of water/MeCN (95:5 v/v); the resulting solution was subjected to reversed-phase analytical chromatography with a preconditioned C18 cartridge (Agilent; 20 mL of immobile phase). The fractions were analyzed by mass spectrometry, the purest ones were col-

lected, and the solvents were removed in vacuo to yield a red resin. The resin was recrystallized by the liquid/liquid diffusion of diethyl ether into a saturated MeCN solution at 4 °C to yield red-brown microcrystals (0.13 g, 14%). C₂₆H₃₃B₂F₈FeN₈O_{3.5}S (775.1): calcd. C 40.2, H 4.2, N 14.4; found C 40.4, H 3.8, N 14.1. MS (ESI): *m/z* (%) = 287.1 (100) [M]²⁺.

Complex 2: The same procedure was applied with 2*H*-1,2,3-triazole and 5-nitrothiophene-2-carbaldehyde to yield red-brown crystals (0.12 g, 12.5%) suitable for X-ray diffraction analysis. C₂₅H₃₄B₂F₈FeN₉O_{4.5}S (794.1): calcd. C 37.8, H 4.3, N 15.8; found C 37.7, H 4.0, N 15.5. MS (ESI): *m/z* (%) = 287.5 (100) [M]²⁺.

Complex 3: The same procedure was applied with 1*H*-pyrazole and 5-nitrofuran-2-carbaldehyde to yield a red-brown microcrystalline powder (90 mg, 10%). Attempts to crystallize the powder from MeCN solutions were unsuccessful; the powder was used for subsequent studies. C_{26.5}H_{32.5}B₂Cl_{1.5}F₈FeN₈O₄ (809.7): calcd. C 39.3, H 4.0, N 13.8; found C 39.1, H 3.7, N 13.5. MS (ESI): *m/z* (%) = 279.1 100 [M]²⁺.

Complex 5: The same procedure was applied with 1,2-benzopyrazole and 5-nitrofuran-2-carbaldehyde to yield red-brown crystals (0.10 g, 10%) suitable for X-ray diffraction analysis. C₃₄H₃₈B₂F₈FeN₁₀O₃ (864.2): calcd. C 47.3, H 4.4, N 16.2; found C 47.2, H 4.2, N 16.4. MS (ESI): *m/z* (%) = 304.1 (100) [M]²⁺.

X-ray Crystallography: Crystals of **2** and **5** were selected and mounted on a Gemini kappa-geometry diffractometer (Agilent Technologies UK, Ltd.) equipped with an Atlas CCD detector and a Mo-K α graphite-monochromated radiation source ($\lambda = 0.7107$ Å). The intensities were collected at low temperature with the CrysAlis-Pro software to a maximum 2θ value of 59.2°.^[33] Reflection indexing, unit-cell parameter refinement, Lorentz polarization correction, peak integration, and background determination were performed. An analytical absorption correction was applied by using the modeled faces of the crystal.^[34] The crystal parameters and details of the data collection are summarized in the Supporting Information. The structures were solved by direct methods with SIR97.^[35] and the least-square refinement on F^2 was achieved with the CRYSTALS software.^[36] All non-hydrogen atoms were refined anisotropically. The hydrogen atoms were all located in a difference map, but those attached to carbon atoms were repositioned geometrically. The H atoms were initially refined with soft restraints on the bond lengths and angles to regularize their geometry (C··H in the range 0.93–0.98 and N··H in the range 0.86–0.89 Å) and $U_{\text{iso}}(\text{H})$ values (1.2–1.5 times the U_{eq} values of the parent atom), after which the positions were refined with riding constraints.

CCDC-989146 (for **2**) and -989147 (for **5**) contain the supplementary crystallographic data for this paper. These data can be obtained free of charge from The Cambridge Crystallographic Data Centre via www.ccdc.cam.ac.uk/data_request/cif.

Magnetic Moment Determination: The solution-phase magnetic moments of **1–3** and **5** were determined by the Evans method with the Schubert refinement.^[21,22] For each complex, a pure sample was dissolved in H₂O/D₂O (90:10) containing an additional 2% *t*BuOH. The frequency shift of the *t*BuOH NMR signal between this solution and that of a reference was measured in situ by using a coaxial NMR tube; the corresponding magnetic moments of the complexes were calculated from the frequency shifts. The formulas, calculation parameters, and additional information are summarized in Figure S13 and Table S2.

T₁ Measurements: The longitudinal relaxation times (T_1) of the protons of the water molecules in aqueous solutions of **1–3** and **5** were determined by NMR spectroscopy. For each complex, a pure

sample was dissolved in the indicated solvent containing an additional drop of D₂O. The ¹H NMR spectra of the solution were acquired by using an inversion–recovery sequence with increasing recovery times τ . The area of the NMR signal of the water protons, a , is proportional to the total magnetization of the water protons in the solution and was extracted for each spectrum and plotted against τ . The T_1 values were calculated by fitting this curve with the exponential function $a(\tau) = a_0(1 - e^{-\tau/T_1})$.

Activation Experiments:^[8] Pure samples of **1–3** or **5** were dissolved in PBS (50 mM, pH 7.4) to give 4 mM solutions. Pd/C (10% w/w, 0.1 equiv.) was added, and hydrogen gas was bubbled through the suspension with a needle for 5–10 min until the total reduction of the complex was observed by mass spectrometry. The solution was filtered and subsequently incubated at 37 °C. The activation was monitored by MS, UV/Vis spectroscopy, T_1 measurements, and Evans NMR spectroscopy measurements.

Supporting Information (see footnote on the first page of this article): MS spectra; X-ray structural analyses; UV/Vis spectra; NMR spectra; solution-phase magnetic moment measurements; UV monitoring of the robustness of **11** in PBS; monitoring of robustness, conversion, and fragmentation by MS; and NMR and UV/Vis monitoring of fragmentation.

Acknowledgments

F. T. and C. G. thank the French Ministère de la Recherche for PhD fellowships. A postdoctoral fellowship to Y. B. by the Bullukian Foundation, Lyon, France is gratefully acknowledged. Erwann Jeanneau is thanked for performing the X-ray structural analyses.

- [1] Committee on Revealing Chemistry through Advanced Chemical Imaging, National Research Council of the national Academies, *Visualizing Chemistry: The Progress and Promise of Advanced Chemical Imaging*, National Academies Press, Washington DC, **2006**.
- [2] M. P. Shores, C. M. Klug, S. R. Fiedler, in: *Spin-Crossover Materials* (Ed.: M. A. Halcrow), Wiley, Oxford, UK, **2013**, p. 281.
- [3] B. Weber, in: *Spin-Crossover Materials* (Ed.: M. A. Halcrow), Wiley, Oxford, UK, **2013**, p. 55.
- [4] P. B. Tsitovich, J. A. Spornyak, J. R. Morrow, *Angew. Chem. Int. Ed.* **2013**, *52*, 13997–14000; *Angew. Chem.* **2013**, *125*, 14247.
- [5] J. Hasserodt, WO 2005/094,903, **2005**.
- [6] V. Stavila, M. Allali, L. Canaple, Y. Stortz, C. Franc, P. Maurin, O. Beuf, O. Dufay, J. Samarut, M. Janier, J. Hasserodt, *New J. Chem.* **2008**, *32*, 428–435.
- [7] J. Hasserodt, J. L. Kolanowski, F. Touti, *Angew. Chem. Int. Ed.* **2014**, *53*, 60–73; *Angew. Chem.* **2014**, *126*, 60.
- [8] F. Touti, P. Maurin, J. Hasserodt, *Angew. Chem. Int. Ed.* **2013**, *52*, 4654–4658; *Angew. Chem.* **2013**, *125*, 4752.
- [9] A. R. Katritzky, X. F. Lan, J. Z. Yang, O. V. Denisko, *Chem. Rev.* **1998**, *98*, 409–548.
- [10] H. Lepaumier, D. Picq, P.-L. Carrette, *Ind. Eng. Chem. Res.* **2009**, *48*, 9061–9067.
- [11] D. Coucouvanis, in: *Inorganic Syntheses*, Wiley, New York, **2002**, *33*.
- [12] K. Wiegardt, E. Schoffmann, B. Nuber, J. Weiss, *Inorg. Chem.* **1986**, *25*, 4877–4883.
- [13] L. Christiansen, D. N. Hendrickson, H. Toftlund, S. R. Wilson, C. L. Xie, *Inorg. Chem.* **1986**, *25*, 2813–2818.
- [14] L. Spiccia, G. D. Fallon, M. J. Grannas, P. J. Nichols, E. R. T. Tiekink, *Inorg. Chim. Acta* **1998**, *279*, 192–199.
- [15] M. C. Lopez, R. M. Claramunt, P. Ballesteros, *J. Org. Chem.* **1992**, *57*, 5240–5243.
- [16] P. Ballesteros, R. M. Claramunt, M. C. Lopez, J. Elguero, G. Gomez-Alarcon, *Chem. Pharm. Bull.* **1988**, *36*, 2036–2041.
- [17] P. Ballesteros, J. Elguero, R. M. Claramunt, *Tetrahedron* **1985**, *41*, 5955–5963.
- [18] M. C. Gallego-Preciado, P. Ballesteros, R. M. Claramunt, M. Cano, J. V. Heras, E. Pinilla, A. Monge, *J. Organomet. Chem.* **1993**, *450*, 237–244.
- [19] S. J. Dorazio, P. B. Tsitovich, S. A. Gardina, J. R. Morrow, *J. Inorg. Biochem.* **2012**, *117*, 212–219.
- [20] F. S. Boig, G. W. Costa, I. Osvar, *J. Org. Chem.* **1953**, *18*, 775–778.
- [21] D. F. Evans, *J. Chem. Soc.* **1959**, 2003–2005.
- [22] E. M. Schubert, *J. Chem. Educ.* **1992**, *69*, 62–62.
- [23] I. Parveen, D. P. Naughton, W. J. Whish, M. D. Threadgill, *Bioorg. Med. Chem. Lett.* **1999**, *9*, 2031–2036.
- [24] S. A. Everett, M. A. Naylor, K. B. Patel, M. R. Stratford, P. Wardman, *Bioorg. Med. Chem. Lett.* **1999**, *9*, 1267–1272.
- [25] S. Ferrer, D. P. Naughton, M. D. Threadgill, *Tetrahedron* **2003**, *59*, 3437–3444.
- [26] Z. Li, X. Li, X. Gao, Y. Zhang, W. Shi, H. Ma, *Anal. Chem.* **2013**, *85*, 3926–3932.
- [27] X. P. Qian, O. Hindsgaul, *Chem. Commun.* **1997**, 1059–1060.
- [28] F. Touti, P. Maurin, L. Canaple, O. Beuf, J. Hasserodt, *Inorg. Chem.* **2012**, *51*, 31–33.
- [29] J. D. Chapman, A. P. Reuvers, J. Borsa, A. Petkau, D. R. McCalla, *Cancer Res.* **1972**, *32*, 2616–2624.
- [30] J. M. Berry, C. Y. Watson, W. J. D. Whish, M. D. Threadgill, *J. Chem. Soc. Perkin Trans. 1* **1997**, 1147–1156.
- [31] N. P. Mahmud, S. W. Garrett, M. D. Threadgill, *Anti-Cancer Drug Des.* **1998**, *13*, 655–662.
- [32] R. F. Borch, J. Liu, J. P. Schmidt, J. T. Marakovits, C. Joswig, J. J. Gipp, R. T. Mulcahy, *J. Med. Chem.* **2000**, *43*, 2258–2265.
- [33] *CrysAlisPro*, version 1.171.34.49, Agilent Technologies, **2011**.
- [34] R. C. Clark, J. S. Reid, *Acta Crystallogr., Sect. A* **1995**, *51*, 887–897.
- [35] A. Altomare, M. C. Burla, M. Camalli, G. L. Cascarano, C. Giacovazzo, A. Guagliardi, A. Moliterni, G. Polidori, R. Spagna, *J. Appl. Crystallogr.* **1999**, *32*, 115–119.
- [36] P. W. Betteridge, J. R. Carruthers, R. I. Cooper, K. Prout, D. J. Watkin, *J. Appl. Crystallogr.* **2003**, *36*, 1487–1487.

Received: December 12, 2014

Published Online: ■

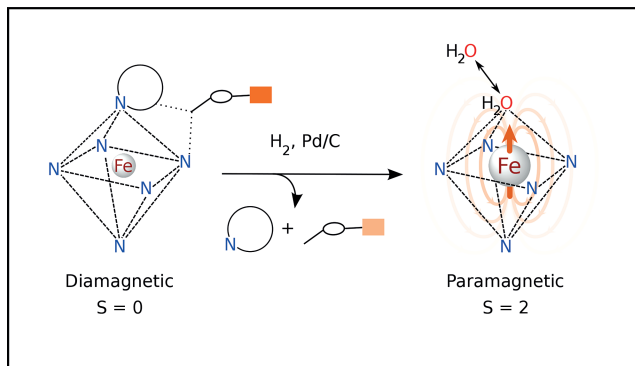
Magnetogenic Probes

C. Gondrand, F. Touti, E. Godart,
Y. Berezhansky, E. Jeanneau, P. Maurin,
J. Hasseroth* 1–8



Spring-Loaded Iron(II) Complexes as
Magnetogenic Probes Reporting on a
Chemical Analyte in Water

Keywords: Cage compounds / Iron / Mag-
netic properties / Macrocyclic ligands / N
ligands



A new low-spin iron(II) triazacyclononane-based complex, selected from four different candidates, acts as a molecular probe that turns a diamagnetic aqueous sample into a paramagnetic one as a response to a chemi-

cal analyte. The four complexes are prepared by a highly convergent synthetic protocol and give precious insights into structure–activity relationship (SAR) tendencies.